LOSSES EVALUATION IN CONVERTERS USING THE CALORIMETRIC TECHNIQUE

Kaiçar Ammous[1], *Bruno Allard*[2], *Hatem Garrab*[2] *and Anis Ammous*[1*]

[1]Groupe Electronique de Puissance (PEG), ENIS-Sfax, Département de Génie Electrique, BPW 3038 Sfax, Tunisie
[2]Centre de Génie Electrique de Lyon, CNRS UMR5005, INSA-Lyon, Bâtiment Léonard de Vinci, F-69621 Villeurbanne Cedex, France

In this paper, a measurement technique of losses in the switching cell, based on calorimetric technique is presented. A special calorimeter was designed to be able to access the heat generated by an operating converter. Power component losses are studied according to the cyclic ratio and to operating frequency and an extraction method of the different terms of these losses, using calorimetric measurements, is presented.

An accurate expression of the switching losses in the power semiconductors devices is proposed.

Introduction

The industry of converters has the tendency to manufacture converters more and more compact. With this type of integrated power, the design prototypes become increasingly difficult. For this reason, it is more and more often necessary to refers to the simulation of converters including their thermal part [1] or the EMC pollution [1]. Unfortunately the cost of this long time-range simulation is too high for CAE if accurate semiconductor device models are used [2]. Practically the switching power device constrain the integration time-step to a small value [3]. A classical simplification is possible when using ideal switches instead of semiconductor device models. The simulation cost is only slightly reduced while it does no longer include the semiconductor device effects and non linearity. Another level of simplification is to use an averaged model of the converter including the semiconductor devices non linearity [1, 4]. The losses measurement or estimation is an essentially part of the design and conception.

The reliability of power converters implies that the operating temperature of the semiconductor devices is accurately monitored during the operation of the converter. In fact the monitoring is not implemented and a largely over-designed thermal system is the only insurance for the converter reliability. An effective device temperature is estimated only for security purpose in case of critical operations of the converter (overload, short-circuit…). The direct estimation of a device junction temperature is not yet a mature technique. So the estimation of the device temperature is related to the estimation of the device losses, and an accurate knowledge of the thermal path.

On one hand during the design of the converter thermal path, the design engineer needs an accurate but affordable model of the converter that estimates the converter losses [1] under various operating conditions [1]. On the other hand the improvement of the converter prototype requires the device losses to be measured accurately [5–7].

The indirect estimation of power losses of a power semiconductor device during transients requires the measurement of the current and voltage waveforms. The multiplication of the two waveforms is then integrated over the transient time interval.

Experimentally, the technique uses voltage and current probes. Unfortunately these last deform measurement waveforms.

It is shown that the measured waveforms are not simply a delay between voltage and current waveforms, but overshoots and distortions are introduced by the probes, that may not be corrected easily [3]. Another method is to measure directly and then with accuracy the converter losses under test to be able to validate the diagrams of correction.

So a correction has to be applied to the integration result. Confidence in the latter correction is related to the possibility to compare the numerical results to accurate experimental results. It is then an important issue to be able to measure directly and accurately the losses of a converter under operation [6–8].

Experimental results on the losses of a power converter are key data for the validation of the converter models used for the design of the converter thermal system.

The paper presents the design of a calorimetric system for the direct measurement of power converter

*   Author for correspondence: anis.ammous@enis.rnu.tn

losses. The cost of a calorimetric system renders the prototyping approach unaffordable.

In the first part of the paper we have presented the principal and the characteristics of the realized of the calorimeter prototype. In the second part, an experimental technique using the calorimeter is used to the evacuated energy by a DC–DC converter. The chosen converter is based on a switching cell including a power Mosfet and a diode. The proposed technique allowes the evolution of the total losses of the total switching cell. In the third part of the paper analytics study's and experimental measurement are used to identify the dissipated power in conduction states of each components as a function of the switching period and the duty ratio. Switching losses evolution as function of direct magnitude and for a given applied voltage and duty ratio is deduced too.

Prototype description

We need to perform heat flow measurement on a real operating converter, that means a large volume. It is then impossible to ensure strict adiabatic conditions. Wires to supply the converter represent unavoidable thermal losses that degrade the system adiabaticity [4]. It has been necessary to adapt an isothermal calorimeter [6–8], and adapt a measurement technique. Figure 1 depicts the principle of our calorimeter. A sufficiently insulated pot contains the converter

(the device under test), a calibration resistance and a temperature sensor. The pot is filled with a liquid to distribute heat and adjust a thermal capacitance. For dielectric insulation purpose, the pot is filled with oil. The pot is placed inside an isothermal water tub. The volume of the tub is over-sized compared to the pot, in order to achieve the isothermal assumption, at least during the measurements. A waterproof cover seals the pot, but manages enough space for the connecting wires to the converter, the calibration resistance and the temperature sensor. It is assumed that the generated heat is distributed uniformly and instantaneously inside the pot: a mechanical agitator will be required that is not represented in Fig. 1.

To have a good thermal homogeneity, the pot is filled by oil (thermal driver and electrical insulator). The quantity of oil defines the value of the capacity of the pot C_{pot}. Thermal resistance $R_{lateral}$ represents the interface between the pot and the bucket.

- The pot is a cylinder made of Pyrex glass. It is sealed with a teflon cover.
- The pot is located inside a cylindrical metal can. The purpose of the can is two folds. First, with a sufficiently large diameter, a space filled with air is managed around the pot, that procures thermal insulation. The can diameter defines the thermal resistance $R_{lateral}$, in Fig. 2. Second, the metal can supports the mechanical agitator and its motor, while
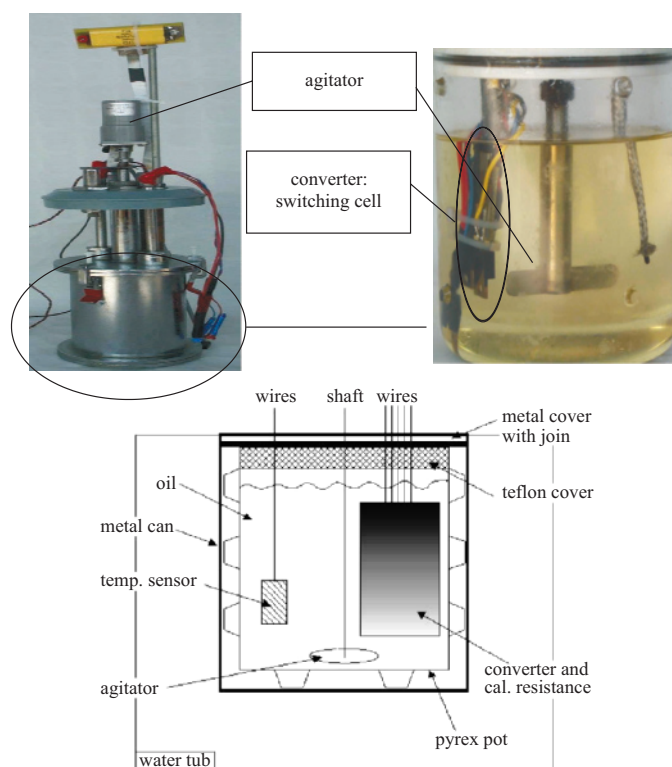

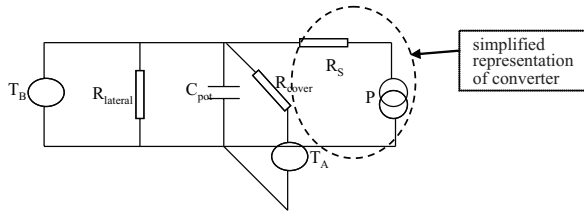**Fig. 1** Technological description of the calorimeter prototype

Fig. 2 The calorimeter model adapted to a switching cell

insuring waterproofness for the pot. The agitator performs the fast diffusion of heat inside the pot.

- The temperature sensor is a semiconductor thermistance. Though non-linear, it is one of the most sensitive thermal devices. A 5 kΩ thermistance features a sensitivity of more than $100\ \Omega\,K^{-1}$ in (300, 400 K) range. A 4-wire configuration enables to detect 0.001 K. An accurate calibration gives the evolution of the device resistance *vs.* temperature.

- The pot is filled with oil. The quantity of oil defines at first order the value of the capacitance C_{pot} in Fig. 2. The order of magnitude of energy lost by the converter under test imposes a range of value for C_{pot} with respect to the Dickinson method. As the volume of the converter imposes the minimal diameter of the pot, the geometrical parameters of the pot are then clearly defined. The volume of air that remains over the oil under the cover is an important part of the thermal resistance, R_{cover}, with regard to the ambient temperature in Fig. 2.

- The calibration resistance is made of two-paralleled 10 Ω/50 W devices in TO-220 packages. The package offers a large heat dissipation surface for a small volume. The resistance power has been chosen quite small, as we want first to test the calorimeter sensitivity, with an efficient test converter (low losses).

- The test converter (switching cell) is described below. It is located in the pot. Many wires connect the different parts inside the pot, to power supplies or measurement instruments (Figs 2 and 3).

- T_A and T_B represent respectively the ambient and water tube (in cylindrical metal) temperature.

- P represents the power losses evacuated by the switching converter.

Experimental investigations for a converter energy losses evaluation

It is supposed that produced heat is distributed uniformly inside the pot: a mechanical agitator is installed. The chosen DC–DC converter is buck converter based on a simple switching cell [9, 10]. A MOSFET and diode are used to represents the switching cell (Fig. 3). The converter is located in the
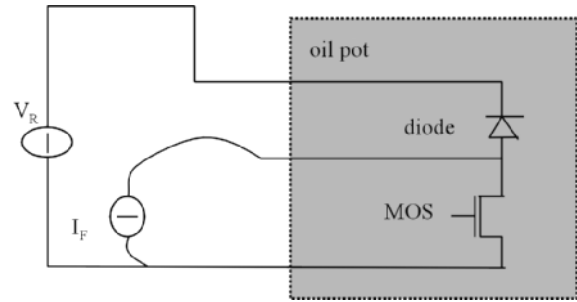

Fig. 3 Electrical circuit: switching cell

oil pot. V_R and I_F are respectively the supply voltage and direct current.

Before switching cell losses measurements, a calibration phase, of the calorimeter is necessary. The used calibration technique is based on a resistance losses measurement. Both the value of the resistance and the magnitude of the current flowing on it are known.

When heat is created by the operation of the converter, or the calibration resistance, it is expected [11–13] a response of the temperature sensor as pictured in Fig. 4a. The temperature inside the pot is initially $T_O < T_B$. Due to the tub higher temperature, the pot temperature, T, increases quite linearly if the capacitance C_{pot} is large enough but not too much. The heat generation (either converter or calibration resistance) creates a brutal increase in the temperature T. When the heat generation stops, the pot temperature, T, increases linearly again. If several operating conditions that are discussed later, are respected, then the temperature variation, ΔT, due to the converter or the calibration resistance, is related to the generated heat flow, Q, by Eq. (1)

$$Q = C\Delta T \qquad (1)$$

where C is the global effective capacitance of the pot, seen by the temperature sensor.

This effective thermal capacitance is related to the geometrical parameters of the pot, the arrangement of the parts inside the pot, and the key temperatures T_A, T_B and T_o. The measurement of the loss energy, Q, is a 2-step process:

- A controlled energy, Q_1, is created through the calibration resistance with a monitored current and a defined duration.

  A variation, ΔT_1, is sensed, and Eq. (1) gives C.

$$C = \frac{Q_1}{\Delta T_1} \qquad (2)$$

The converter is then operated, and the response of the temperature sensor gives the temperature variation, ΔT_2. The loss energy, Q_2, is computed as
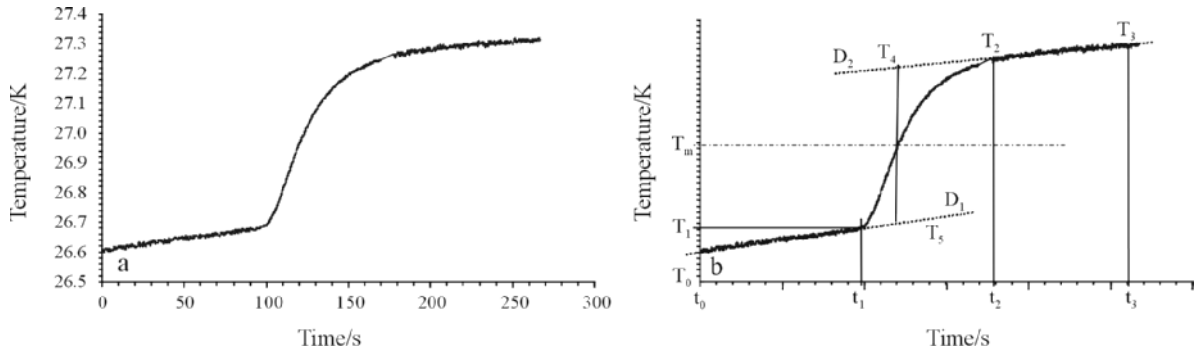
$$Q_2 = C\Delta T_2 \qquad (3)$$

Fig. 4 Typical response of the a – temperature sensor inside the pot, b – Dickinson graphical method
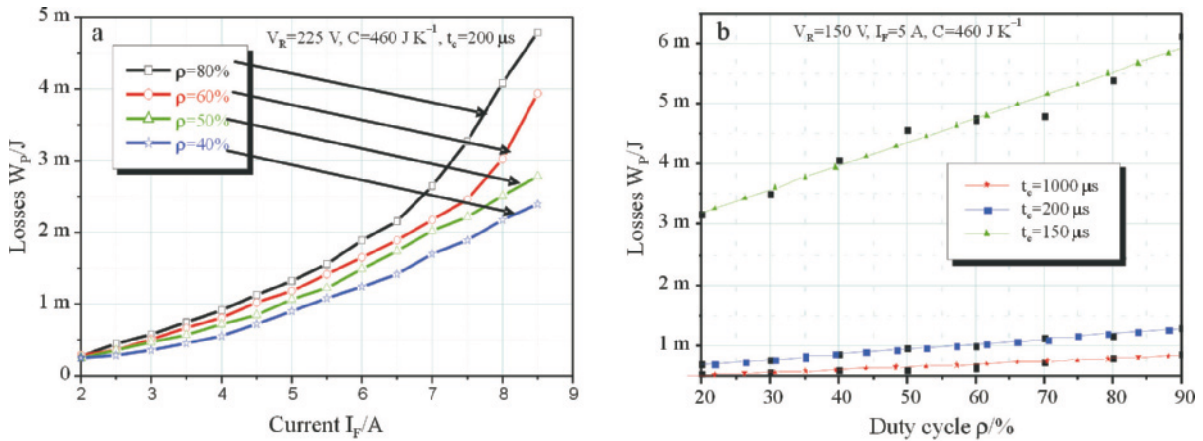

Fig. 5 Experimental losses function of a – direct current and b – duty ratio

The temperature variation, ΔT_2, is determined using the Regnault-Pfoundier equations [11, 12] based on the First and Second Law Thermodynamics. For practical reason, we preferred the Dickinson graphical method [12, 14]. The converter or the calibration resistance, creates heat that is detected as the temperature variation

$$\Delta T = T_2 - T_1 - \Delta T_{cor} \qquad (4)$$

where T_2 and T_1, are the temperatures determined as in Fig. 4b, and ΔT_{cor} is a correction accounting for all the phenomena injecting heat along with the device under test. Basically the temperature, T_m, is evaluated as

$$T_m = \frac{T_2 + T_1}{2} \qquad (5)$$

The straight lines D_1 and D_2 are extrapolated from the temperature gradient over $[t_0, t_1]$ and $[t_2, t_3]$ respectively. At time t_1, the device under test is operated. By time t_2, the effects of heat generation by the device are no more visible. The line D_m, (crossing T_4 and T_5) is the shortest line between D_1 and D_2 that crosses the point of temperature T_m. The temperature variation, ΔT, is then evaluated as

$$\Delta T = T_5 - T_4 \qquad (6)$$

The efficiency of the Dickinson method is related to two main assumptions. First the heat generation must be short compared to the overall experience duration, i.e. $[t_0, t_3]$ in Fig. 4b. Second the temperature gradients over $[t_0, t_1]$ and $[t_2, t_3]$ must be small but significant compared to the heat flow generated by the converter or the calibration resistance. The temperature gradients depend on the pot thermal insulation, and the temperatures T_B and T_0. Finally temperature gradients and temperature variation, ΔT, are directly dependent on the pot capacitance, C_{pot} in Fig. 2.

Experimental results are registered with a switching cell composed with a MOSFET (IRF740) and a diode (BYT12PI600).

Figure 5a shows the evolution of the energy evacuated by the converter as a function of the direct current magnitude for different ratio (ρ) values. This evolution seems to be proportional to the square of the current I_F.

Figure 5b shows the evacuated energy evolution as function of the duty ratio (ρ) for a different period (t_c) values.

The evolution of the cell losses as a function of period duration t_c for different duty ratio value and direct current magnitude are shown in Fig. 6a and b respectively. These evolutions are quite linear.
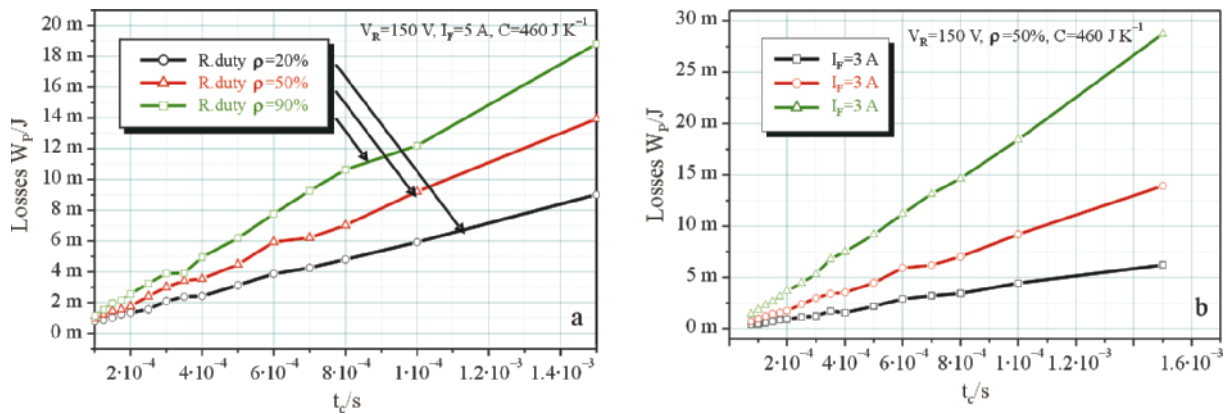
Fig. 6 Measurement losses according to the period t_c and for a – different duty ratio and b – different current value

Losses analysis

In this section we have to develop the expression of the total losses W_p, of the switching cell, as a function of the duty ratio, the period t_c, the dissipated power in 'on' and 'off' states and the losses during the switching phases W_{sw}. Using this expression and the characteristics shown in Fig. 5, we can deduce the different losses (P_{on}, P_{off} and W_{SW}^1) used in this expression.

Figure 7 shows the evolution of the dissipated power in the active device when the MOSFET is driven by a periodic signal. The energy loss $W_{p,MOS}$ is expressed during the period t_c.
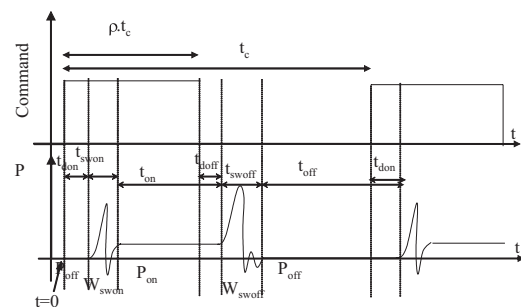

Fig. 7 Mosfet driving command and the power evolution dissipated in the device component

Table 1 The used parameters and their signification

Symbols	Signification (Fig. 7)	Dependence with			
		V_R	I_F	ρ	t_c
V_{MOS}	Component voltage (MOSFET)		*		
i_{MOS}	Current through the component (MOSFET)		*		
i_D	Current through the component (diode)		*		
V_D	Component voltage (diode)	*	*		
P	Power losses in the component	*	*	*	*
t_c	Cyclic period				*
t_{don}	Delay according to the 'off' state to the 'on' state	*	*		
t_{swon}	Switching time according to 'off' state to the 'on' state	*	*		
t_{on}	The on state time duration			*	*
t_{doff}	Delay according to the 'off' state to the 'on' state	*	*		
t_{swoff}	Delay according to the 'on' state to the 'off' state	*	*		
t_{off}	The 'off' state time duration			*	*
W_{swon}	The provided losses during t_{swon}	*	*		
W_{swoff}	The provided losses during t_{swoff}	*	*		
P_{on}	Power losses during 'on' state		*		
P_{off}	Power losses during 'off' state	*			
W_p	Losses during a period t_c, $W_P = \int_0^{tc} p(t)\mathrm{d}t$	*	*	*	*
W_{sw}^1	The sum of the losses provided during the switching times t_{swoff} and t_{swon} ($W_{ton}+W_{toff}$)	*	*		

Table 1 shows the different parameters and variables used to develop the expression of losses W_p.

The dependences of these variables as function of the controls parameters (V_R, I_F, ρ, t_c) are indicated too.

The energy $W_{p,MOS}$ during the period t_c is given by the integral of the dissipated power in the MOSFET during this period as following:

$$W_{p,MOS} = \int_0^{t_c} p(t)dt = \int_0^{t_c} i_{MOS}(t)V_{MOS}(t)dt \qquad (7)$$

Using the evolution of the dissipated in the MOSFET shown in the Fig. 7 and the defined variables listed in Table 1, the energy W_p can be written as:

$$W_{p,MOS} = W_{swon} + P_{on,MOS}t_{on} + W_{swoff} + P_{off,MOS}t_{off} \qquad (8a)$$

We define $W_{sw}^1 = W_{swon} + W_{swoff}$ so, the Eq. (8a) gives:

$$W_{p,MOS} = P_{on,MOS}t_{on} + P_{off,MOS}t_{off} + W_{sw}^1 \qquad (8b)$$

In the last expression we can see the sum of the three terms corresponding to the energy evacuated during the on state (t_{on}), the off state (t_{off}) and during switching phases.

In order to use the characteristics evolution shown in Fig. 5 and corresponding to the total energy losses evacuated by the switching cell, both MOSFET and diode evacuated energy should be expressed as a function of the duty ratio and the operating period t_c.

We define t_{sw} as:

$$t_{sw} = t_{swon} + t_{swoff} \qquad (9)$$

$$t_{on_1} = t_{swon} + t_{don} - t_{doff} \qquad (10)$$

So the on state duration is given by:

$$t_{on}\rho t_c - t_{on_1} \qquad (11)$$

and the off state duration is given by:

$$t_{off} = (1-\rho)t_c + t_{on_1} - t_{sw} \qquad (12)$$

We define W_{SW} as:

$$W_{sw} = W_{sw}^1 - P_{on,MOS}t_{on_1} + P_{off,MOS}[t_{on_1} - t_{sw}] \qquad (13)$$

The last equation shows that the evacuated energy W_{sw} is different from the evacuated energy W_{SW}^1 which is the sum of the switching losses during conduction and blocking phases ($W_{swon} + W_{swoff}$).

Using Eqs 11, 12 and 13 the expression given in Eq. 8b can be written as following:

$$W_{p,MOS} = P_{on,MOS}(i_F)\rho T_c$$
$$+ P_{off,MOS}(V_R)(1-\rho)T_c + W_{sw,MOS}(i_F, V_R) \qquad (14)$$

We notice that the evacuated energy during switching phases W_{sw} can be written as:

$$W_{SW,MOS}(i_F, V_R) = [\int_{t_{don}}^{t_{don}+t_{swon}} (i(t)v(t) - P_{on,MOS})dt] +$$

$$[\int_{\rho_T t_{doff}}^{\rho_T t_{doff}+t_{swoff}} (i(t)v(t) - P_{off,MOS})dt] + \qquad (15)$$

$$(t_{don} - t_{doff})(P_{off,MOS} - P_{on,MOS})$$

The last Eq. (15) allows the real switching losses evaluation from experimental measurement.

How to identify the different losses part using the measurement of $W_{p,MOS}$ as a function of t_c and ρ?

From Eq. (14), W_p can be written as $W_{p,MOS}=At_c+B$, where A and B are constant.

$$P = \frac{W_{p,MOS}}{t_c} = P_{on,MOS(i_F)}\rho +$$

$$P_{off,MOS(V_R)}(1-\rho) + \frac{W_{sw,MOS(i_F,V_R)}}{t_c} \qquad (16)$$

At a given duty ratio ρ and for different switching period values t_{c_1} and t_{c_2} Eq. (14) can be written as following:

$$\frac{W_{p_2,MOS}}{t_{c_2}} - \frac{W_{p_1,MOS}}{t_{c_1}} = \frac{W_{sw,MOS}}{t_{c_2}} - \frac{W_{sw,MOS}}{t_{c_1}} = W_{sw,MOS}\left(\frac{1}{t_{c_2}} - \frac{1}{t_{c_1}}\right)$$

So the switching losses can be deduced from experimental characteristics as:

$$W_{sw,MOS} = \frac{1}{t_{c_2} - t_{c_1}}(t_{c_1}W_{p_2,MOS} - t_{c_2}W_{p_1,MOS}) \qquad (17)$$

For a constant switching period t_c and for two data ratio ρ_1, ρ_2, the dissipated power in the ON state phase can be written as:

$$P_{on,MOS} = \left(\frac{W_{p_2,MOS} - W_{p_1,MOS}}{t_c}\right)(1/(\rho_1 - \rho_2)) \qquad (18)$$

We notice that the dissipated power in OFF state phase (P_{off}) is neglected.

The last study can be applied to the diode in order to determine the different device losses.

Switching cell losses analysis

In this section we have to determine the global losses expression in the case of the switching cell. As it is precise in the last section, Eq. (14) can be written for any active devices and diode in the switching cell (MOSFET and diode in our case).

In Table 2 we have listed the different energy and power symbols, for a given device X.

Table 2 Different energy and power symbols for a given device X

Symbols	Significations
$W_{p,X}$	Energies lost during a period in the component X
$W_{on,X}$	Energies lost on the On state in the component X
$W_{off,X}$	Energies lost on the Off state in the component X
$W_{sw,X}$	Energies lost during switching in the component X
$P_{on,X}$	The losses during the On state for in component X
$P_{off,X}$	The losses during the Off state in the component X

Using Eq. (14), the diode losses is given by:

$$W_{P,Diode} = P_{on,Diode}*(1-\rho)t_c + P_{off,Diode}*(\rho)*t_c + (W_{sw,Diode}) \quad (19)$$

The total loss in the switching cell can be written as:

$$W_P = W_{P,MOS} + W_{P,Diode} = [P_{on,MOS}(\rho) + P_{on,Diode}(1-\rho) + P_{off,MOS}(1-\rho) + P_{off,Diode}(\rho)]t_c + [W_{sw,Diode} + W_{sw,MOS}] \quad (20)$$

We pose:

$$W_{sw} = W_{sw,MOS} + W_{sw,Diode} \quad (21)$$

The ON and the OFF states losses of the diode and the MOSFET are given by the following expressions, respectively.

$$W_{on} = [P_{on,Diode}(1-\rho) + P_{on,MOS}(\rho)]t_c \quad (22)$$

$$W_{off} = [P_{on,MOS}(1-\rho) + P_{on,Diode}(\rho)]t_c \quad (23)$$

Using Eqs (21)–(23), the total switching cell is given by:

$$W_P = W_{on}(i_F) + W_{off}(V_R) + W_{sw}(i_F, V_R) \quad (24)$$

When the duty ratio value is near 1, the active device operates much longer than the diode, so the OFF and the ON states dissipated power in the diode can be neglected. When replacing ρ by 1 in the Eq. (20) we obtain:

$$W_P(\rho=100\%) = W_{P,MOS} + (W_{sw,Diode} + W_{sw,MOS}) = P_{on,MOS}t_c + (W_{sw,MOS} + W_{sw,Diode}) \quad (25)$$

In the same manner when the duty ratio value is near 0, the active device operates much longer than the diode, so the OFF and the ON states dissipated power in the MOSFET can be neglected. When replacing ρ by 0 in the Eq. (20) we obtain:

$$W_P(\rho=0\%) = (W_{P,Diode} + W_{sw,Diode}) = P_{on,Diode}t_c + (W_{sw,Diode} + W_{sw,MOS}) \quad (26)$$

The waveform in the Fig. 5b can be interpolated by a linear strait as $W_P = A\rho + B$.

We appropriate the two particular points of the strait for $\rho=1$ and for $\rho=0$. The found values are repre-

Table 3 Deduced losses W_p for three switching period

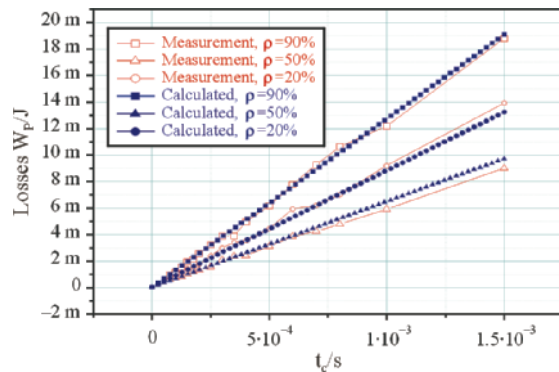| Period	$W_P(\rho=0\%)$	$W_P(\rho=100\%)$
$t_c=150$ μs	0.424 mJ	0.928 mJ
$t_c=200$ μs	0.526 mJ	1.4 mJ
$t_c=1000$ μs	2.48 mJ	6.4 mJ

sented at the Table 3 for different values of period t_c (voltage $V_R=150$ V and direct current $I_F=5$ A).

To determine the dissipated power in the switching cell, characteristics in Fig. 5b can be used in fact. The evolution in the total losses W_p of the switching cell as a function of the duty ratio ρ is approximatively linear. The interpolation of the different linear function at $\rho=0$ and $\rho=1$ allows the determination of the dissipated power in MOSFET and diode at a different switching period t_c. Table 3 resumes the deduced losses W_p for three switching period values.

Equations (25) and (26) and Table 3 allows the determination of the dissipated power in the two devices. For example, for a load current I_F equal to 5 A and a DC voltage $V_R=250$ V, we deduce the dissipated power and the switching energy losses in the diode and MOSFET given in Eqs (17) and (18).

Replacing the last parameters values in the Eq. (2) leads to obtain the expression of the total losses of the switching cell as a function of the switching period t_c and the duty ratio ρ.

Figure 8 shows the deduced evolution of these losses as a function of the period t_c for different duty ratio ρ.

Fig. 8 Comparison of the total losses W_p obtained by measurement and calculation ($I_F=5$ A, $V_R=150$ V)

These deduced evolutions are compared with those obtained by experiment. We note a good concordance between the two types of evolution.

Really the switching losses in the diode and the MOSFET are inseparable but theoretically it is possible to separate them while prolonging the line in Fig. 5b at the top and at the bottom to have the rate cyclic ρ values 1 and 0, respectively.

From Table 3 and Eqs (25), (26), we can deduct the values of $P_{on,MOS}(i_F)$ and $P_{on,Diode}(i_F)$ for a voltage and current V_R=150 V and I_F=5 A functionnement. So,

$$P_{on,Diode}(i_F)=4.85(\text{J s}^{-1}),\ W_{sw,Diode}=38.02\ (\mu\text{J})\quad(27)$$

$$P_{on,MOS}(i_F)=12.70(\text{J s}^{-1}),\ W_{sw,MOS}=50.18\ (\mu\text{J})\quad(28)$$

From the last study and using the experimental characteristics shown in Fig. 6, the evolution of the switching losses as a function of a direct current and at a given applied voltage and duty ratio can be deduced, this evolution is shown in Fig. 9.
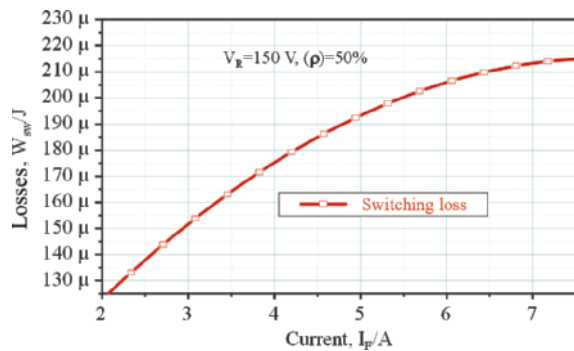

Fig. 9 Evolution of the switching losses, $W_{sw,}$ in the diode according the direct current I_F

Conclusions

In this paper we have presented an experimental technique to evaluate total losses evacuated by a given converter. In our case the used converter is based in a switching cell composed by a MOSFET and diode. In order to evaluate the dissipated power in each component of the switching cell using the experimental results, a theorical analysis is performed for these reasons, using the obtained analytical expression and the experimental results. The dissipated power in conduction states of each component is evaluated. Switching losses are evaluated too as a function of direct current at a given applied voltage and duty ratio.

For a given device, the performed study allows the estimation of the evolution of the dissipated power in this components as a function of the switching period and the duty ratio, using experimental investigations.

Nomenclature

A: effective area
n: electron density
ND: doping density
p: hole density
q: electronic charge
$Q_{n,p}$: charge (for *n,p*-type semiconductor)
W_b: base width
x_n: depletion layer width in an *n*-type semiconductor
ρ: charge density per unit volume
τ_n: electron lifetime
τ_p: hole lifetime
ε: dielectric constant of the semiconductor
ut: thermal voltage
SCR: space charge region
Γ: the net doping concentration

References

1 A. Ammous, M. Ayedi, Y. Ounajjar, K. Ammous and H. Morel, Eur. Phys. J., (2003).
2 H. Morel, S. H. Gamel and J. P. Chante, Device Equation: A Novel Approach. IEEE Transaction on Power Electronics, Janury 94, Vol. 9, No. 1. pp. 112–120.
3 K. Ammous, B. Allard, O. Brevet, H. Elomari, D. Bergogne, D. Ligot, René Ehlinger and H. Morel, Proceedings of IEEE PESC 2000, Vol. 1, pp. 212–218.
4 B. Allard, H. Morel, K. Ammous, X. Lin-Shi, D. Bergogne, O. Brevet and P. Bevilacqua, International conference of bond graph modeling, ICBGM 2001, pp. 264–270.
5 K. Ammous, A. Ammous, B. Allard and H. More, Smart Systems and Devices 2000, pp. 158–162.
6 M. A. A. O'Neil, S. Gaisford, A. E. Beezer, C. V. Skaria and P. Sears, J. Therm. Anal. Cal., 84 (2006) 301.
7 M. A. Kuznetsov and S. I. Lazarev, J. Measurement Techniques, 48 (2005) 8.
8 S. Tomitaka, M. Mizukami, F. Paladi and M. Oguni, J. Therm. Anal. Cal., 81 (2005) 637.
9 K. Ammous, B. Allard, H. Morel and A. Ammous, International conference of bond graph modeling, ICBGM 2003.
10 K. Ammous, B. Allard, A. Ammous and H. Morel, EPF2000, pp. 107–109.
11 J. P. McCullogh and W. Scott, Vol. 1, London, Butterworths 1968, p. 606.
12 T. D. McGee, Principles and Methods of Temperature Measurements, John Wiley, New York 1988, p. 581.
13 G. N. Lewis and M. Randall, Thermodynamics, McGraw-Hill, New York 1961, p. 723 (Series in Advanced Chemistry).
14 B. Allard, Contribution aux méthodes et outils de conception des systèmes (intégrés) de puissance, INSA Lyon, Habilitation à diriger des recherches en sciences, 2001.